The Potential Regenerative Effect of L-carnitine Pretreated Mesenchymal Stem Cells in Myocardial Infarction Through Modulating Apoptosis, Inflammation, and Cellular Differentiation

Abir El Sadik *, Hamad M. Alsaykhan , Jihad Awad Alrehaili , Abdullah saleh Alkhamiss , Ahmed Elzainy

Posted Date: 28 May 2024

doi: 10.20944/preprints202405.1819.v1

Keywords: Inflammation; tissue regeneration; apoptosis; ischemic heart disease; cell proliferation.

Article

The Potential Regenerative Effect of L-Carnitine Pretreated Mesenchymal Stem Cells in Myocardial Infarction through Modulating Apoptosis, Inflammation, and Cellular Differentiation

Abir El Sadik [1,*], Hamad M. ALsaykhan [2], Jihad Awad Alrehaili [3], Abdullah Saleh Alkhamiss [4] and Ahmed Elzainy [5]

[1,5] Department of Anatomy and Histology, College of Medicine, Qassim University, Buraydah 52571, Saudi Arabia and Department of Anatomy and Embryology, College of Medicine, Cairo University, Cairo, Egypt
[2] Department of Anatomy and Histology, College of Medicine, Qassim University, Buraydah 52571, Saudi Arabia; h.alsaykhan@qu.edu.sa; ahmedelzainy@qu.edu.sa
[3] Department of Pathology, College of Medicine, Imam Mohammad Ibn Saud Islamic University (IMSIU), Riyadh 11564, Saudi Arabia; jaalrehaili@imamu.edu.sa
[4] Department of Pathology, College of Medicine, Qassim University, Buraydah 52571, Saudi Arabia; 3772@qu.edu.sa
* Correspondence: abeer.ouaida@kasralainy.edu.eg

Abstract: Preconditioned mesenchymal stem cells (MSCs) represent an advanced method to overcome the challenges related to their survival rate, differentiation, and activity maintenance. L-carnitine has demonstrated antioxidant and anti-apoptotic effects on injured cardiac cells. However, limited research has been conducted to explore their combined effect on cardiac tissue injury. Therefore, the present study aimed to conduct a comparative and comprehensive study investigating the role of L-carnitine-pre-treatment on the immunomodulation of inflammation, apoptosis, and differentiation of MSCs and their impact on cardiac toxicity induced by Doxorubicin (DOX). Rats were divided into group I (control), group II (DOX), group III (DOX+MSCs), group IV (DOX+L-carnitine), group V (DOX+L-carnitine pre-treated MSCs). CK-MB, troponin I, MDA, and catalase levels were improved in the treated groups (III, IV, and V). The degeneration and necrosis of the cardiomyocytes were reduced in the treated groups. They regained their normal architecture in the L-carnitine pre-treated MSCs group. These findings were augmented by analyzing the immunomodulators; NF-κβ, TNFα, and IL-1β, the proliferative indicators Ki-67, and hsp90, the cardiac differentiation marker TH and the apoptotic regulators; caspase 3 and Bcl2. These results demonstrate the optimal regenerative and therapeutic effects of L-carnitine pre-treated MSCs representing an efficient tool for future stem cell therapy.

Keywords: inflammation; tissue regeneration; apoptosis; ischemic heart disease; cell proliferation

1. Introduction

Cardiovascular diseases are recognized as the leading causes of morbidity and mortality globally [1,2]. The worldwide incidence rate of myocardial infarction is very high and continues to rise each year [3,4]. The treatment of myocardial infarction primarily relies on swift reperfusion and reopening of the blocked vessels to save injured cardiomyocytes, reduce infarct size, and restore myocardial tissue [5–7]. Cancer drug therapy is one of the principal sources of cardiac side effects and cancer therapy-related cardiac dysfunction (CTRCD) [8–10]. One of these chemotherapeutic drugs is Doxorubicin (DOX). DOX is an effective anthracycline-wide-ranging chemotherapeutic drug that has garnered significant attention. It is used to treat multiple types of cancer, such as breast and

 doi:10.20944/preprints202405.1819.v1

oesophageal cancers, Kaposi's sarcoma, osteosarcoma, acute lymphocytic leukemia, bladder cancer, and Hodgkin's and non-Hodgkin's lymphomas [11–13]. However, it is considered a mixed blessing because of its severe dose-dependent cardiotoxicity. The toxicity of DOX damages the cardiac muscle fibers and eventually results in pathological dilated cardiomyopathy [14,15]. The dilated cardiac chambers significantly reduce the ventricular ejection fraction (EF). Consequently, it affects the contractile function and leads to heart failure [16,17]. The cardiac muscles are particularly vulnerable to DOX toxicity due to their high mitochondria-to-cardiomyocyte ratio, which increases susceptibility to oxidative stress [18–20]. Doxorubicin induces vascular endothelial damage. The main mechanism underlying this toxicity involves the overproduction of reactive oxygen species (ROS). This excessive ROS generation can produce mitochondrial dysfunction, harming the vascular endothelium [21,22]. Endothelial cell injury is associated with subsequent infiltration of leukocytes and secretion of cytokines such as interleukin (IL)-1β, IL-6, and tumor necrosis factor-α (Tnf- α) [23,24]. These cytokines have important functions in the body's immune response, such as activating and recruiting leukocytes to areas of inflammation. However, excessive production of these cytokines can produce an intensified inflammatory response, potentially causing cardiac tissue damage. In addition, DOX produces overexpression of nuclear factor kappa-B (NF-κβ) and reduction of the antiapoptotic protein; B-cell lymphoma 2 (Bcl2) which stimulates the apoptotic cascade [25,26].

Recent research indicates that mesenchymal stem cells (MSCs) have the potential to improve the regeneration of injured cardiomyocytes. Beyond their ability to proliferate and differentiate, MSCs can also generate several immunoregulatory factors that modulate the inflammation and immune responses in the cardiac microenvironment that directly initiate the therapeutic process [27–29]. However, targeted migration, low survival rates, poor differentiation, and sustaining MSC activity in the injured tissue pose significant challenges that impact their effectiveness as a regenerative therapy. The number of cells and passages, culture conditions, delivery methods, chemo-attractants released from damaged tissue, host conditions, effective inter-cellular communication, and the microenvironment of injured tissue collectively influence the homing, survival, bioavailability, and effectiveness of MSCs. Several studies suggested that alterations in the microenvironment of the injured region, including oxidative stress, hypoxia, acidosis, inflammation, and insufficient nutrients hinder stem cells from effectively engaging in the regeneration processes [30–32]. To address these limitations, recent research recommends employing a strategy known as "cell preconditioning." Cell preconditioning stands out as a promising modality that enhances the tolerance and therapeutic capacity of transplanted cells, using specific non-stress-inducing agents, such as drugs, cytokines, chemokines, growth factors, and various biological mediators, that initiate numerous signaling pathways to assist stem cells at the site of injury [33–35]. One of these preconditioning factors is the L-carnitine.

L-carnitine (3-hydroxy-4-N-trimethylammonium-butyrate), an amino acid derivative and a potent antioxidant, exerts various biological effects. It is crucial for the β-oxidation of fatty acids in mitochondria to produce adenosine triphosphate, which also plays a significant role in various mitochondrial functions [36,37]. Recent studies investigated the therapeutic efficacy of preconditioning of MSCs with L-carnitine in the field of regenerative medicine [38]. Fathi et al. [39] detected that L-carnitine can enhance neurogenesis from MSCs through the Wnt/β-catenin and PKA signaling pathways. L-carnitine extends the life span of MSCs, reduces population doubling time and aging, enhances fatty acid metabolism, and decreases lipid peroxidation. These findings were reported by Mobarak et al. [40] when evaluating the effects of L-carnitine on the proliferation and aging of MSCs derived from rat adipose tissue. L-carnitine has been investigated for its potential protective effects in heart ischemia-reperfusion injury. It reduced the levels of proinflammatory cytokines and restored the expression of antioxidative genes such as SOD1, SOD2, and SOD3. It significantly lowered elevated Bax expression and caused an increase in Bcl-2 expression, leading to a favorable adjustment in the Bcl-2/Bax ratio [41]. Additionally, L-carnitine plays multiple protective roles against cardiac injury in isoprenaline-treated myocardial infarction rat models by suppressing oxidative stress by reducing ROS and enhancing endogenous antioxidant enzyme functions. In addition, it demonstrated significant cardioprotective effects as evidenced by decreased infiltration

 doi:10.20944/preprints202405.1819.v1

of inflammatory cells and the inhibition of TNF-α and IL-1β [2]. Other studies explored the anti-apoptotic effects of L-carnitine in heart failure. L-carnitine inhibited pro-apoptotic protein expression such as caspases, decreased levels of TNFα and its second messenger sphingosine, and reduced the number of apoptotic myonuclei [42]. Although most studies explored the beneficial effects of L-carnitine against cardiotoxicity through its anti-inflammatory, antioxidant, and antiapoptotic influence, limited research has been conducted to investigate the effects of pre-treatment of MSCs with L-carnitine and their combined impact on cardiac tissue injury.

2. Materials and Methods

2.1. Preparation, Labeling, and Pre-Treatment of MSCs

Bone marrow (BM)-MSCs were isolated and cultured at the Biochemistry and Molecular Biology Unit, Faculty of Medicine, Cairo University. Bone marrow was collected by flushing the femurs and tibiae of 6-week-old male rats with DMEM (Sigma, St. Louis, MO, USA, D5796) supplemented with 10% fetal bovine serum (Sigma, St. Louis, MO, USA, F6178). The cells were layered over Ficoll-Hypaque (Sigma, St. Louis, MO, USA, F8016) in sterile conical tubes at a 2:1 ratio and then centrifuged. The nucleated cells were isolated and resuspended in a complete culture medium supplemented with 1% penicillin-streptomycin (Sigma, St. Louis, MO, USA, P4333). The primary culture was maintained by incubating the cells at 37 °C in 5% humidified CO2 for fourteen days, with the media completely replaced every four days. Once the cells reached 80% confluence and large colonies had formed, the cultures were washed twice with PBS (Sigma, St. Louis, MO, USA, P5493). The cells were then trypsinized using 0.25% trypsin (Sigma, St. Louis, MO, USA, T1426) in 1 mL EDTA (Sigma, St. Louis, MO, USA, E6758) for five minutes at 37 °C and centrifuged at 2400 rpm for 20 minutes. For the first passage, the cell pellets were suspended and incubated in 25 cm^2 culture flasks. MSCs were identified based on their morphology, adherence, expression of surface markers (positive for CD34, CD45, CD90, and CD105), and their ability to differentiate into osteocytes and chondrocytes. The MSCs were labeled with PKH26, a red fluorochrome, following the manufacturer's instructions (Sigma, St. Louis, MO, USA) for in vivo cell tracking. Cell viability was assessed by mixing the cell suspension with 0.4% trypan blue stain in a 1:1 ratio. Under a phase contrast microscope, viable cells appeared shiny and unstained [43–45]. 10mM of L-carnitine (Sigma Chemical Company; St Louis, Moment, USA) were added to the stem cells. BM-MSCs were centrifuged and labeled with fluorescent PKH26 (Sigma, USA, MIDI26) for cell tracking after injection [38].

2.2. Experimental Animals

Fifty male *Sprague Dawley* rats were utilized in the current work. The rats weighed from 200 to 250 g. Two weeks for an acclimatization period were given to the rats before the start of the experiment. Access to food and water ad libitum were provided to the animals at room temperature. The experimental animals were handled following the international guidelines for the care and use of laboratory animals. The research proposal was accepted (approval number 23-67-04) by the Committee of Research Ethics, Deanship of Scientific Research, Qassim University. The experimental animals were randomly divided into five groups (with 10 rats in each group):

Group I (control group): 0.5 ml saline intraperitoneal (I.P.) weekly

Group II (Doxorubicin):.5 mg/kg I.P. Doxorubicin (Sigma Chemical Company; St Louis, Moment, USA) weekly [46].

Group III (Doxorubicin and BM-MSCs): 5 mg/kg I.P. Doxorubicin weekly and one systemic injection (through the caudal vein) of stem cells (1 x 10^6) diluted in 0.5 ml of PBS once on day one [43].

Group IV (Doxorubicin and L-carnitine): 5 mg/kg I.P. Doxorubicin weekly and oral L-carnitine (100 mg/kg) daily (Sigma Chemical Company; St Louis, Moment, USA) [2].

Group V (Doxorubicin and BM-MSCs pre-treated with L carnitine): Doxorubicin and one systemic injection (through the caudal vein) of stem cells pre-treated with L carnitine (1 x 10^6) diluted in 0.5 ml of PBS once on day one.

 doi:10.20944/preprints202405.1819.v1

2.3. Biochemical Assays

Blood samples were collected six hours after Doxorubicin administration by retro-orbital plexus technique with capillary glass tubes. The collected blood samples were analyzed for serum cardiac marker enzymes; creatine kinase-myocardial band (CK-MB) and troponin I [47]. At the end of the experiment, on the 28th day, blood samples were collected for enzyme-linked immunosorbent assay (ELISA) investigations. Sandwich ELISA kits (Cloud-Clone Corp., Texas, USA) were used for the assessment of the levels of the apoptotic factor, caspase 3 [48], and the inflammatory and immune regulators, nuclear factor kappa beta (*NF-kβ) [49] and IL 1b [50].*

2.4. Assay of Cardiac Lipid Peroxide Malondialdehyde (MDA) and Antioxidant Enzyme Catalase

The experimental rats received 40 mg/kg pentobarbital I.P. for euthanasia and the heart of each rat was dissected. The cardiac specimens were utilized for colorimetric assessment of lipid peroxide malondialdehyde (MDA) (catalog number MD 25 29) and antioxidant enzyme catalase (catalog number CA 25 17) using the thiobarbituric acid method and H2O2 respectively. The biodiagnostic kits were used following the manufacturer's instructions [51,52].

2.5. Quantitative Real-Time Polymerase Chain Reaction (QRT-PCR)

Cardiac samples (0.2 mg) were homogenized in PBS (pH 7.4) using a TissueLyser (Qiagen, Hilden, Germany) and then centrifuged at 8000× g for 20 minutes. Total RNA was extracted following the manufacturer's protocol using the RNeasy Mini Kit (cat. no. 217004, Qiagen, Hilden, Germany). cDNA was synthesized through reverse transcription using the QuantiTect Reverse Transcription Kit (cat. no. 205311, Qiagen, Hilden, Germany) [53]. The gene expression for tumor necrosis factor-alpha (TNF-α) and B-cell lymphoma 2 (Bcl2) levels was amplified from cDNA using the QuantiTect SYBR Green PCR Kit cat no: 204141 (Qiagen, Germany) and the QuantiTect primer assays cat no: 249900 [(Rn_Tnfrsf1a_1_SG QuantiTect Primer Assay, ID QT00388346), and (Rn_Bcl2_1_SG QuantiTect Primer Assay, ID QT00184863), using the housekeeping gene ACTB as the primer sequence. All samples were analyzed with the 5-plex Rotor-Gene PCR Analyzer (Qiagen, Hilden, Germany) employing the 2ΔΔCt method [44].

2.6. Immunofluorescent Study for Ki-67

The cardiac specimens were fixed in 4% formaldehyde in PBS for 15 minutes at room temperature, then covered with ice-cold 100% methanol and incubated for 10 minutes at −20 °C. The tissue was rinsed in PBS for 5 minutes and then blocked with a blocking buffer for 60 minutes. After aspirating the blocking solution, the anti-Ki-67 Polyclonal Antibody (Invitrogen; ThermoFisher Scientific, Hilden, Germany; Catalogue Number PA5-16785) was applied. The cardiac samples were incubated with a fluorochrome-conjugated secondary antibody, diluted in an Antibody Dilution Buffer, for two hours at room temperature in the dark (Goat anti-rabbit IgG (H + L) Alexa Fluor 488, Invitrogen; ThermoFisher Scientific, Hilden, Germany, Catalogue Number A-11034). The slides were then covered with Prolong® Gold Antifade Reagent (#9071) or Prolong® Gold Antifade Reagent with DAPI (#8961). Microscopic examination was conducted using a LABOMED Fluorescence Microscope LX400 (cat. no. 9126000, NY, USA) with the appropriate excitation wavelength [45].

2.7. Hematoxylin and Eosin (H&E) and Masson's Trichrome Stains

The cardiac specimens were fixed in a 10% formaldehyde solution, processed, and embedded to create paraffin blocks, which were then sectioned at a thickness of 5 µm. The sections were deparaffinized in xylene, rehydrated through a series of alcohol solutions (100%, 95%, and 70%), and finally washed in distilled water. The sections underwent hematoxylin staining for ten minutes, resulting in the basophilic structures of the cytoplasm and nuclei being stained blue. Subsequently, the sections were stained in one percent aqueous eosin for three minutes, which stained the acidophilic structures of the cytoplasm red. Following staining, the sections were dehydrated in

 doi:10.20944/preprints202405.1819.v1

alcohol (70%, 90%, then 100%) and cleared with xylene. Finally, the slides were removed from xylene, mounted in Canada balsam, and covered with a cover slip. Masson's trichrome stain was utilized to evaluate the increase in collagen fibers, indicating fibroplasia. The sections were initially stained in Weigert's iron hematoxylin solution for 10 minutes, followed by rinsing in running tap water for 10 minutes and washing in distilled water. Subsequently, they were stained in Biebrich scarlet-acid fuchsin solution for 15 minutes, washed in distilled water, and differentiated in phosphomolybdic-phosphotungstic acid solution for 10 minutes. The sections were then transferred to an aniline blue solution for ten minutes, briefly rinsed in distilled water, and differentiated in 1% acetic acid solution for five minutes before being rewashed in distilled water. Finally, the sections were rapidly dehydrated in absolute ethyl alcohol, cleared in xylene, and mounted in Canada balsam [53].

2.8. Immunohistochemical Reaction

The cardiac specimens were cut into sections with a thickness of 5 μm and then placed onto slides coated with Poly-L-lysine. These sections underwent deparaffinization in two changes of xylene and were subsequently rehydrated through graded washes of ethanol in water, concluding with a rinse in pure water. Next, they were treated with 0.9% hydrogen peroxide in absolute methanol for 10 minutes. Antigen retrieval was achieved by heating the sections in 10 mm sodium citrate buffer in a water bath at 95°C for 30 minutes. Following this, the sections were rinsed twice in PBS tween 20 for 2 minutes each and then blocked with 5% normal mouse serum for 30 minutes at room temperature [54]. The primary antibodies were incubated for 30 minutes. Heat shock protein 90 (hsp90) beta antibodies were detected by anti-mouse IgG (catalog number: MA1-10892, 1 μg/ml, dilution 1:50, Pittsburgh, Pennsylvania, USA). Tyrosine hydroxylase (TH) antibodies were detected by anti-mouse monoclonal antibodies (catalog number: MA1-24654, 50 μg/ml, dilution 1:100, Pittsburgh, Pennsylvania, USA). Brown discoloration of the cardiomyocytes indicates a positive reaction for the two antibodies.

2.9. Histomorphometric Measurements

An independent observer measured the area percentage of collagen fibers, in Masson's trichrome stain, and the positive immune response in sections stained for HSP90 and TH using a Leica LAS V3.8 image analyzer computer system (Heerbrugg, Switzerland). Systematic sampling was employed by dividing the specimen into a grid and selecting ten non-overlapping fields at a magnification of 400 at regular intervals in a systematic pattern. The area percentage represented the areas of the positive reaction, masked by a binary blue color within a standard measuring frame (7286.783 μm^2), and the area percentage of stained cells was quantified using Cellsens dimension software ver. 4.2 (Olympus, Tokyo, Japan).

2.10. Statistical Analysis

The data of the present study were tabulated and statistically analyzed using personal computers with GraphPad Prism (version 10.1.2) and SPSS 25 (SPSS, Inc., Chicago, IL, USA) software. Analysis of variance using one-way ANOVA and Tukey's honest significance difference (HSD) post hoc test was performed for the comparison between the quantitative variables. Quantitative data were presented in the form of mean and standard deviation (SD). A p-value of <0.05 will be considered statistically significant [55].

3. Results

3.1. Biochemical Results

The mean values of the serum markers enzymes CK-MB and troponin I were significantly increased in the DOX-treated rats, compared with the control group. There was a significant decrease in the mean values of these enzymes in the groups treated with DOX+MSCs, L-carnitine, and L-carnitine-pre-treated MSCs groups (groups III, IV, and V), compared with the DOX-treated group. Regarding the groups treated with MSCs (groups III and V), no significant difference was detected

 doi:10.20944/preprints202405.1819.v1

in relation to the control group (group I). The mean values of caspase 3, NF-κβ, and IL-1β were significantly increased in the DOX-treated rats, compared with the control group. There was a significant decrease in the mean values of these factors in the groups treated with MSCs, L-carnitine, and L-carnitine-pre-treated MSCs groups (groups III, IV, and V), compared with the DOX-treated group with maximum decrease in group V (DOX+L-carnitine-pre-treated MSCs group) ($P < 0.05$) (Table 1, Figure 1).

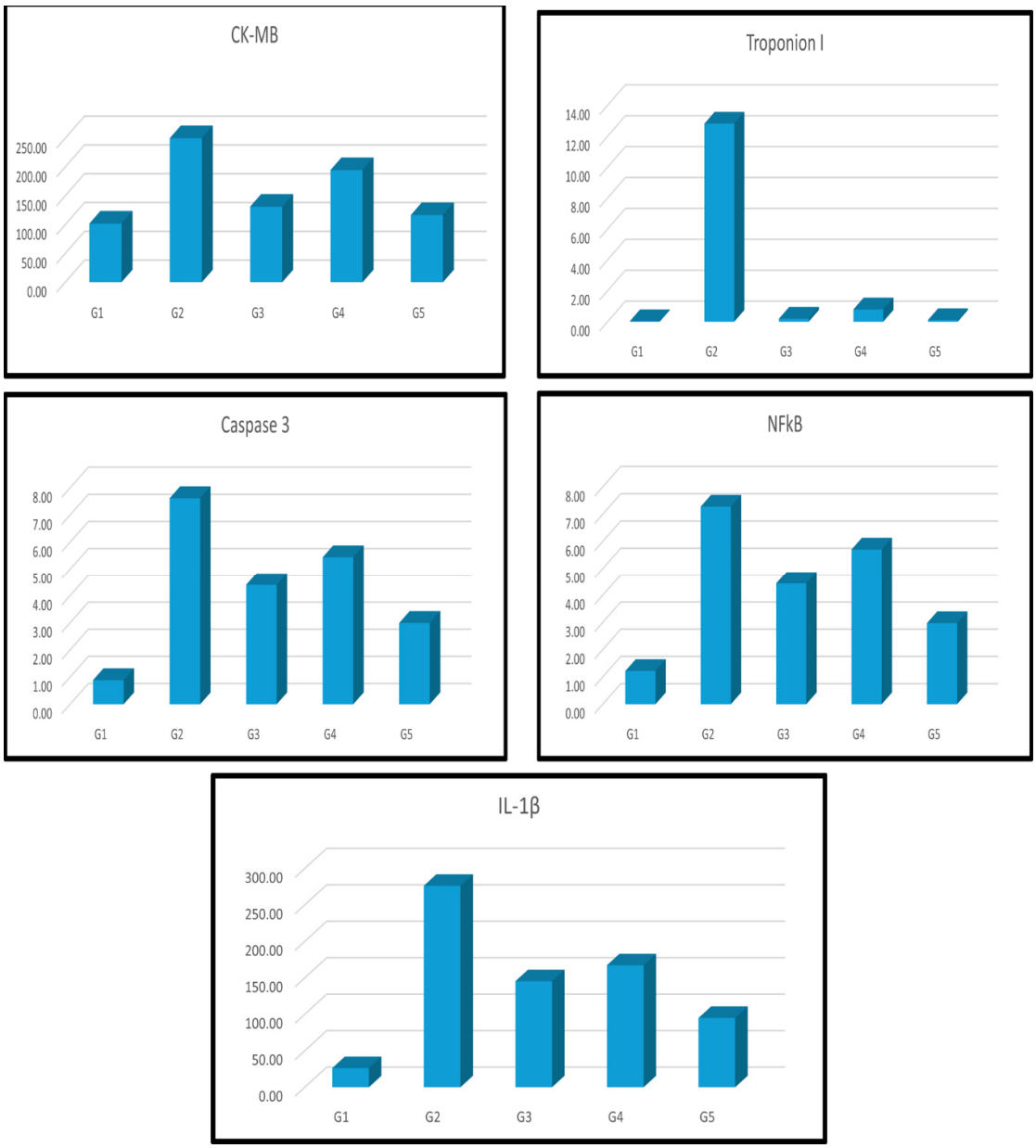

Figure 1. Mean values ± standard deviation of the levels of serum enzymes and ELISA parameters.

Table 1. Mean values ± standard deviation of the levels of serum enzymes and ELISA parameters.

Groups	CK-MB	Troponin I	Caspase 3	NF-κβ	IL-1β
Group I (Control)	1.02±1.78[b]	0.04±0.01[b]	0.89±0.05[b]	1.22±0.07[b]	26.27±1.68[b]
Group II	2.50±9.79[a]	12.81±0.90[a]	7.62±0.37[a]	7.28±0.36[a]	276.24±8.02[a]

 doi:10.20944/preprints202405.1819.v1

(Dox)					
Group III (Dox+MSCs)	1.31±5.11[a b]	0.19±0.06[b]	4.40±0.23[a b]	4.44±0.10[a b]	145.37±6.83[a b]
Group IV (Dox+Lcarnitine)	1.95±5.24[a b]	0.79±0.03[a b]	5.44±0.12[a b]	5.71±0.13[a b]	167.28±7.15[a b]
Group V (Dox+MSCs+Lcarnitine)	1.17±2.44[a b]	0.10±0.01[b]	2.99±0.06[a b]	2.97±0.09[a b]	95.00±3.47[a b]

[a] statistically significant compared with group I, [b] statistically significant compared with group II.

3.2. Assay of MDA and Catalase

The mean values of MDA were significantly increased in the DOX-treated rats, compared with the control group with a significant decrease in the groups treated with DOX+MSCs, L-carnitine, and L-carnitine-pre-treated MSCs groups (groups III, IV, and V), compared with the DOX-treated group and maximum decrease in group V (DOX+L-carnitine-pre-treated MSCs group). Regarding catalase mean values, there was significant decrease in the DOX-treated rats, compared with the control group with a significant increase in the groups treated with DOX+MSCs, L-carnitine, and L-carnitine-pre-treated MSCs groups (groups III, IV, and V), compared with the DOX-treated group and maximum increase in group V (DOX+L-carnitine-pre-treated MSCs group). ($P < 0.05$) (Table 2, Figure 2).

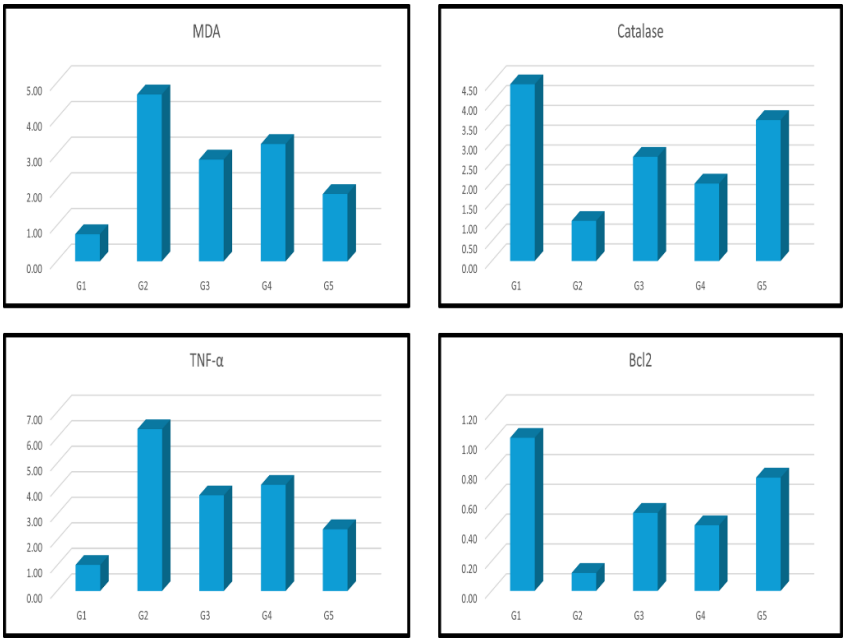

Figure 2. Mean values ± standard deviation of the levels of MDA, Catalase, TNF-α, and Bcl2.

Table 2. Mean values ± standard deviation of the levels of MDA, Catalase, TNF-α, and Bcl2 gene expression.

Groups	MDA	Catalase	TNF-α	Bcl2
Group I (Control)	0.76±0.02[b]	4.47±0.17[b]	1.02±0.33[b]	1.03±0.40[b]
Group II (Dox)	4.68±0.14[a]	1.02±0.07[a]	6.34±0.46[a]	0.12±0.03[a]
Group III (Dox+MSCs)	2.85±0.25[a b]	2.63±0.32[a b]	3.75±0.17[a b]	0.52±0.02[a b]
Group IV	3.29±0.16[a b]	1.96±0.34[a b]	4.16±0.24[a b]	0.44±0.01[a b]

 doi:10.20944/preprints202405.1819.v1

(Dox+Lcarnitine)				
Group V (Dox+MSCs+Lcarnitine)	1.89±0.05[a b]	3.56±0.22[a b]	2.42±0.19[a b]	0.76±0.11[b]

[a] statistically significant compared with group I, [b] statistically significant compared with group II.

3.3. Real-Time PCR for TNF-α and Bcl2 Gene Expression

Detection of mRNA exhibited a significant increase in the expression of TNF-α in the DOX-treated rats, compared with the control group with a significant decrease in the groups treated with DOX+MSCs, L-carnitine, and L-carnitine-pre-treated MSCs groups (groups III, IV, and V), compared with the DOX-treated group and maximum decrease in group V (DOX+L-carnitine-pre-treated MSCs group). Concerning Bcl2 expression, there was significant decrease in the DOX-treated rats, compared with the control group with a significant increase in the groups treated with DOX+MSCs and L-carnitine, and L-carnitine-pre-treated MSCs groups (groups III, IV, and V), compared with the DOX-treated group and maximum increase in group V (DOX+L-carnitine-pre-treated MSCs group). No significant difference was detected in group V (DOX+L-carnitine-pre-treated MSCs group) in relation to the control group (group I). ($P < 0.05$) (Table 2, Figure 2).

3.4. PKH26 Fluorescence Stain and Immunofluorescent Study for Ki-67

Group III (Dox+MSCs) and group V (Dox+MSCs+Lcarnitine) showed PKH26 labeled red fluorescent BM-MSCs in the myocardium with more expression in the L-carnitine pre-treated BM-MSCs group. Regarding Ki-67, the proliferation indicator, samples of the control group showed a moderate yellow-green reaction, while, the Dox-treated group (group II) showed minimal reaction to Ki-67. The specimens of the Dox+MSCs treated group and Dox+Lcarnitine group (groups III and IV) revealed moderate reaction. Dox+MSCs+Lcarnitine group (groups V) revealed increased reaction to Ki-67 (Figure 3A–G).

 doi:10.20944/preprints202405.1819.v1

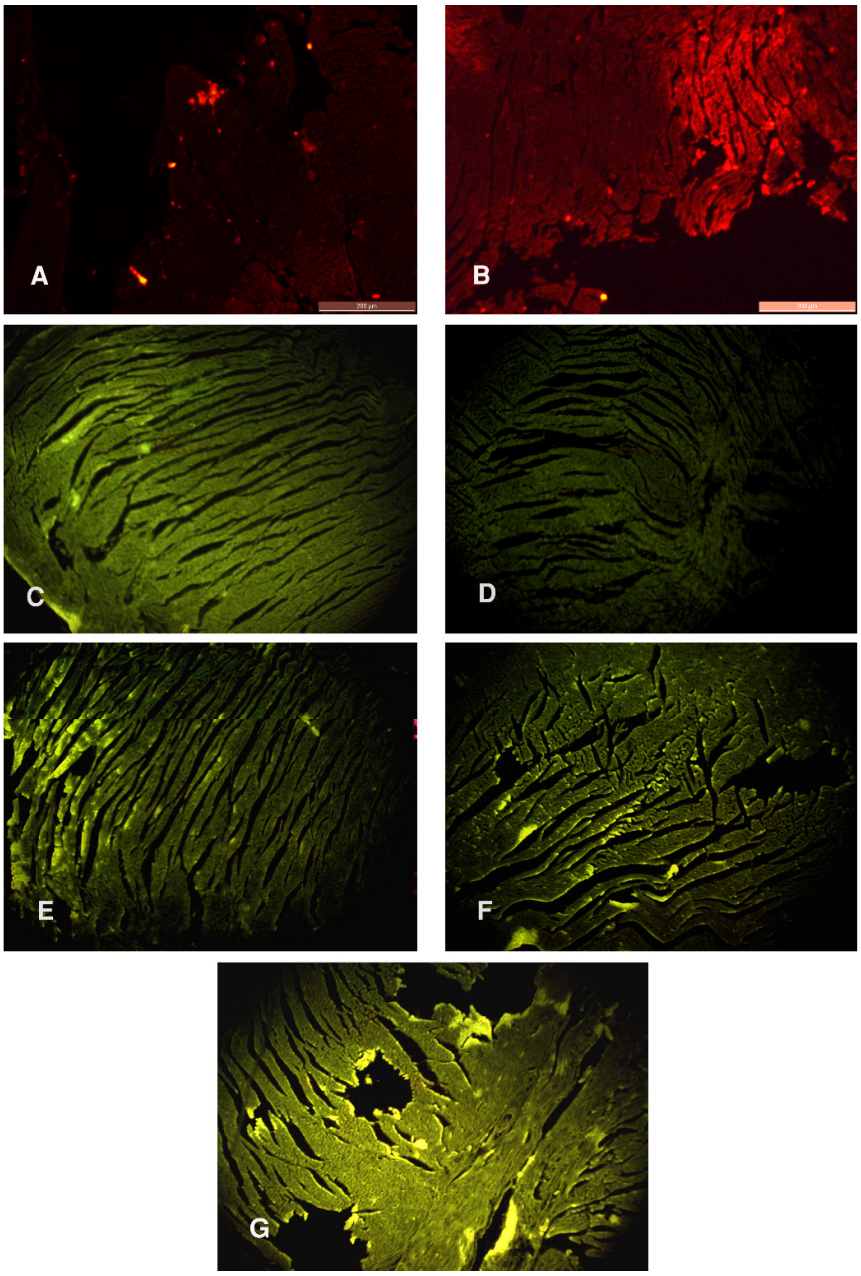

Figure 3. Photomicrographs of the myocardium A) group III and B) group IV showing red fluorescent cells in the myocardium. C) Group I shows a moderate immunofluorescent yellow-green reaction. D) group II shows a minimal immunofluorescent yellow-green reaction. E & F) Groups III & IV show moderate immunofluorescent yellow-green reactions. G) Group V shows increased immunofluorescent yellow-green reactions. (A & B; PKH x100, C-G; Ki-67 x 100).

3.5. Haematoxylin and Eosin Stain

The specimens of the control group showed normal architecture of the cardiomyocytes with branching muscle fibers and normal central vesicular nuclei. Group II (Dox-treated group) revealed fragmented and degenerated cardiomyocytes, separated by empty spaces, congested blood vessels, inflammatory cellular infiltration, pyknotic nuclei, and thickening of the blood vessel walls. Group III (Dox+MSCs treated group) showed normal branched cardiomyocytes separated by a few empty spaces. Group IV (Dox+Lcarnitine group) revealed some empty spaces due to a few fragmented

 doi:10.20944/preprints202405.1819.v1

myocytes and inflammatory cellular infiltration. Group V (Dox+MSCs+Lcarnitine group) showed normal cardiac muscle fibers (Figure 4A–F).

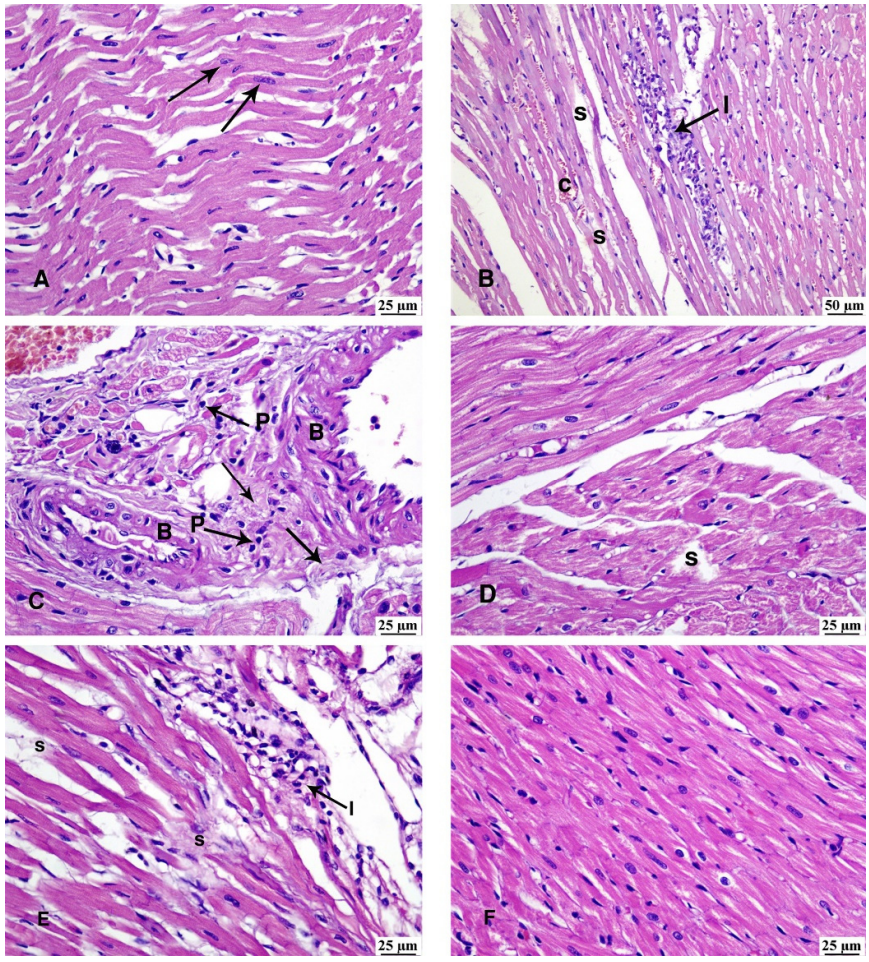

Figure 4. Photomicrographs of the myocardium A) group I showing the normal architecture of the myocardium with branching cardiac muscle fibers with normal central vesicular nuclei (arrows). B and C) Group II showing fragmented and degenerated cardiomyocytes (arrows) separated by empty spaces (S), congested blood vessels (C), inflammatory cellular infiltration (I), pyknotic nuclei (P), and thickening of the blood vessel wall (B). D) Group III shows normal branched cardiomyocytes separated by a few empty spaces (S). E) Group IV shows some empty spaces due to a few fragmented myocytes (S) and inflammatory cellular infiltration (I). F) Group V shows normal cardiac muscles. (H & E: A, C-F x 400, B x 200).

3.6. Masson's Trichrome Stain

Specimens of the control group (group I) showed traces of collagen fibers between the cardiomyocytes. Fibroplasia was detected in Group II (Dox-treated group) and Group IV (Dox+Lcarnitine group). Meanwhile, lower deposition of fibrous tissue was noticed in group III (Dox+MSCs treated group), and traces of collagen fibers were observed in group V (Dox+MSCs+Lcarnitine group) (Figure 5A–F).

 doi:10.20944/preprints202405.1819.v1

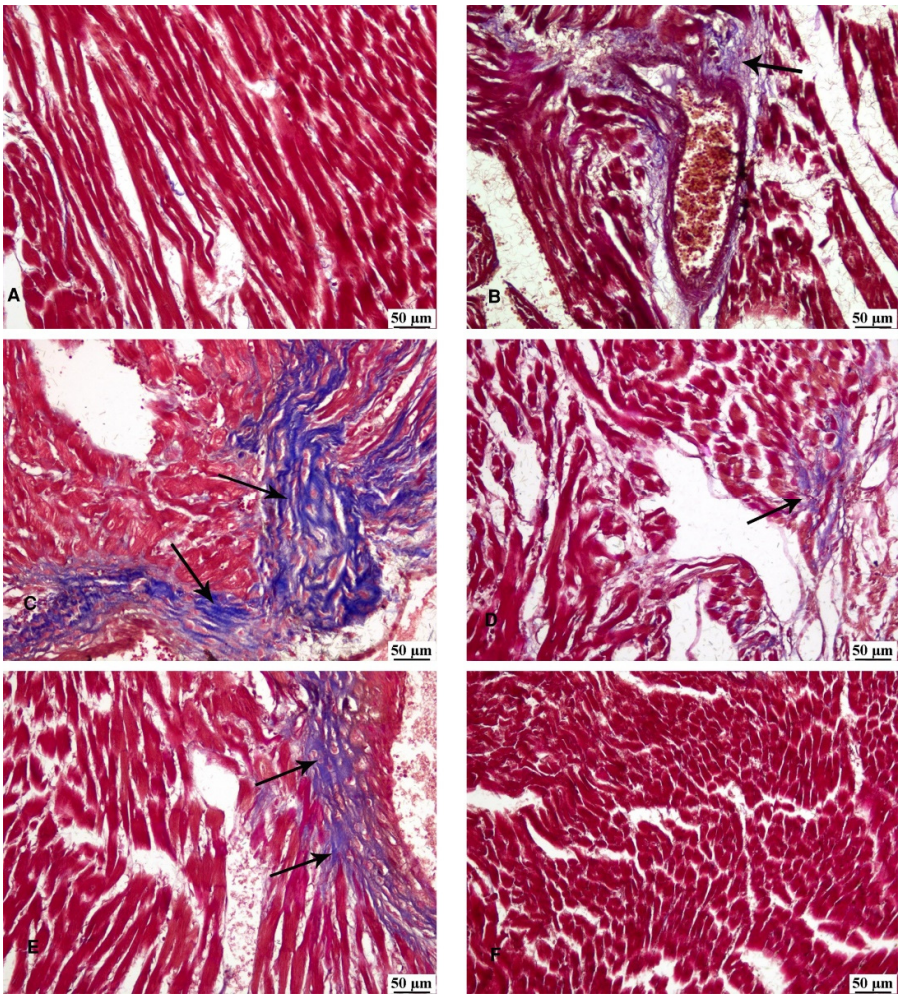

Figure 5. Photomicrographs of the cardiac tissue. A) Group I shows traces of collagen fibers between the cardiomyocytes. B & C) Group II shows fibroplasia around the blood vessels and between the cardiac muscles (arrows). (D) Group III shows a minimal amount of collagen fibers (arrow). (E) Group IV shows fibroplasia (arrow). F) Group V shows traces of collagen fibers. (Masson's trichrome ×200).

3.7. Immunohistochemical Reaction

The specimens of the control group (group I) showed lower expression of hsp90 in the cardiomyocytes of all examined sections. Meanwhile, group II (Dox-treated group) revealed higher expression of hsp90. Moderate expression of hsp90 was noticed in group III (Dox+MSCs treated group). Higher expression of hsp90 was noticed in group IV (Dox+Lcarnitine group) and lower expression was detected in group V (Dox+MSCs+Lcarnitine group) (Figure 6A–F). Regarding the immune reaction to TH, lower TH expression was detected in the control group (group I) and group II (Dox-treated group). Meanwhile, the highest expression of TH was determined in group III (Dox+MSCs treated group) and group V (Dox+MSCs+Lcarnitine group). Moderate TH expression was detected in group IV (Dox+Lcarnitine group) (Figure 7A–E).

 doi:10.20944/preprints202405.1819.v1

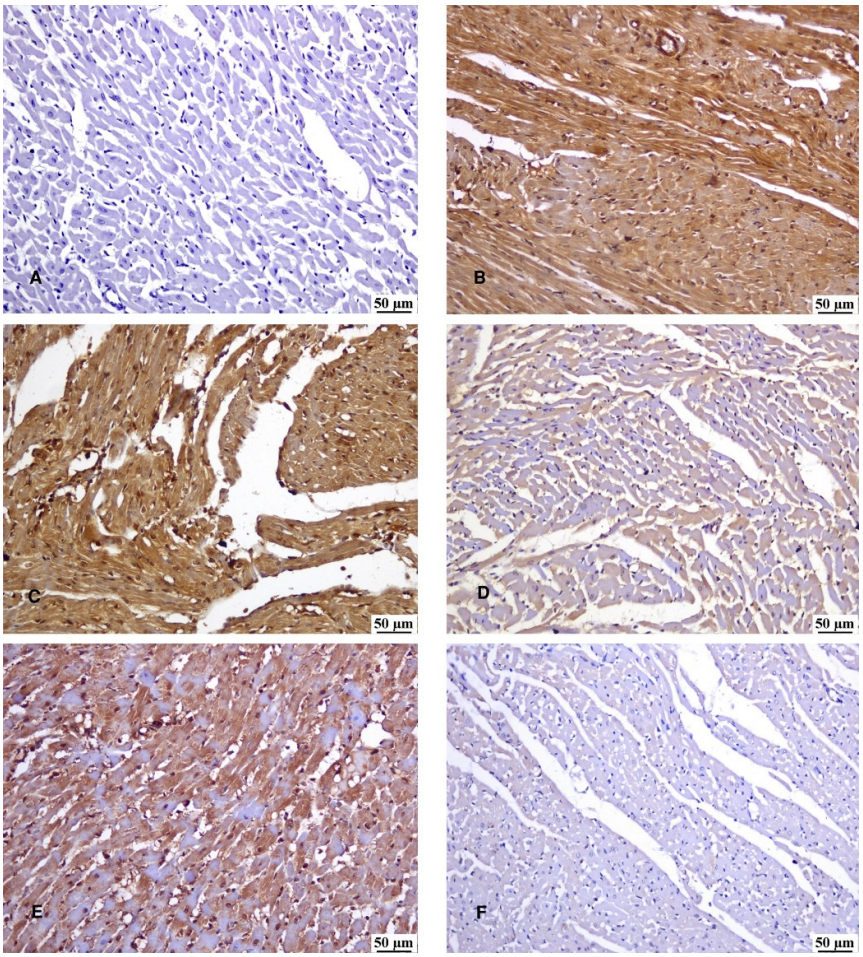

Figure 6. Photomicrographs of the myocardium A) Group I shows weak hsp90 expression. B & C) Group II shows intense hsp90 expression. D) Group III shows moderate hsp90 expression. E) Group IV shows higher hsp90 expression. F) Group V shows lower hsp90 expression. (Hsp90 x 200).

 doi:10.20944/preprints202405.1819.v1

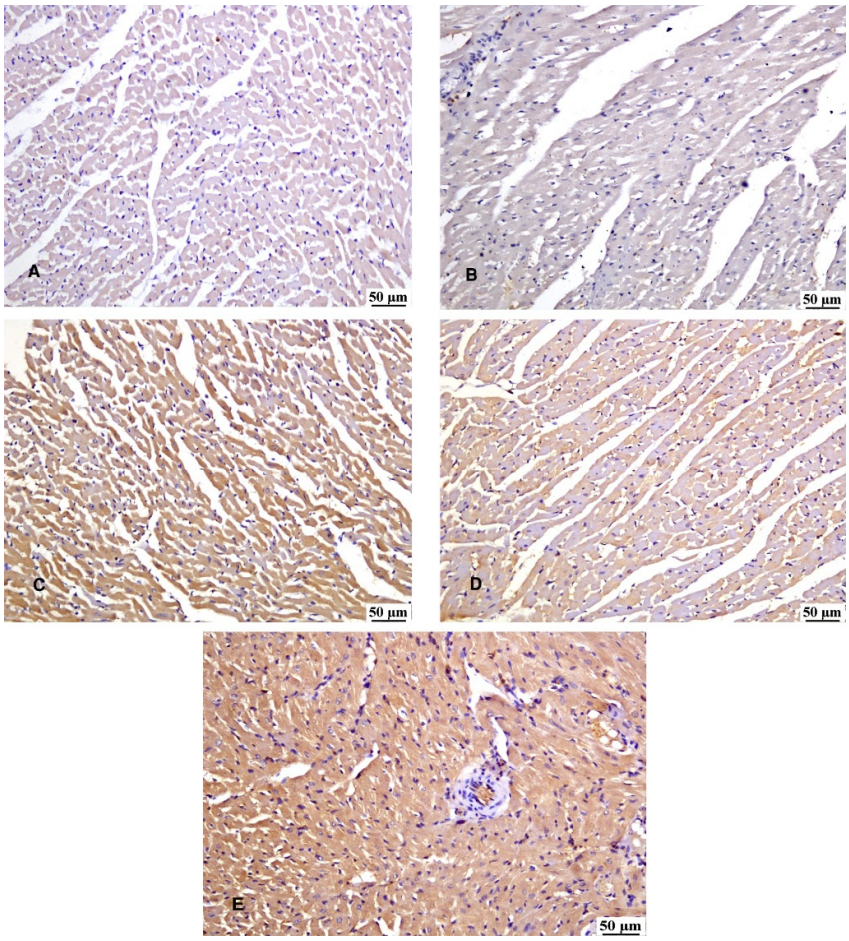

Figure 7. Photomicrographs of the myocardium A & B) Group I and Group II show low TH expression. D) Group IV shows moderate TH expression. C & E) Group III and Group V show higher TH expression (TH x 200).

3.8. Histomorphometric Results

The mean area percent of collagen fibers, in Masson's trichrome stain, was significantly increased in group II (Dox-treated group) and group IV (Dox+Lcarnitine group) in relation to the control group (group I). However, there was a significant decrease of collagen fibers in the groups treated with MSCs; group III (Dox+MSCs treated group) and group V (Dox+MSCs+Lcarnitine group) in relation to group II (Dox-treated group). The mean area percent of hsp90 expression was significantly increased in group II (Dox-treated group) and group IV (Dox+Lcarnitine group) in relation to the control group (group I). However, there was a significant decrease in hsp90 expression in the groups treated with MSCs; group III (Dox+MSCs treated group) and group V (Dox+MSCs+Lcarnitine group) in relation to group II (Dox-treated group). The mean area percent of TH expression was significantly increased in groups III, IV, and V; (Dox+MSCs, Dox+Lcarnitine, and Dox+MSCs+Lcarnitine treated groups respectively) in relation to group I (control group) and group II (Dox-treated group) (Figure 8).

 doi:10.20944/preprints202405.1819.v1

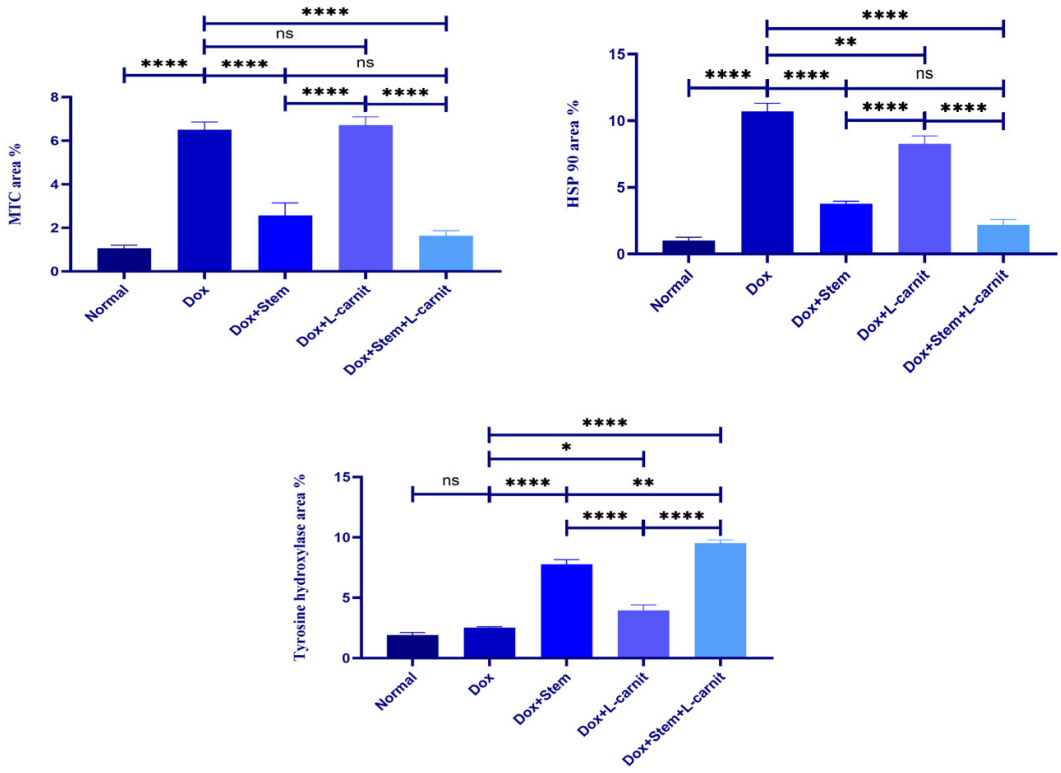

Figure 8. Mean values of the area percent ± standard deviation of Masson's trichrome stain (MTC), HSP90, and TH expression.

4. Discussion

The role of the current conventional therapy of ischemic heart diseases is inadequate to protect against future ischemic events and further myocardial damage or cardiomyocyte regeneration. Unlike MSC therapy, it revealed a decrease in scar size, myocardial fibroplasia, and cardiac function improvement [56–58]. MSCs release a variety of biologically active immunomodulators such as growth factors cytokines, and chemokines, which possess anti-inflammatory, anti-fibrotic, angiogenic, proliferative, and regenerative effects [59,60]. Several studies investigated the effects of MSCs on myocardial infarction. MSCs enhance neovascularization, cardiomyocyte repair, and replacement of dead myocardium in addition to the prevention of myofibril apoptosis [58]. However, the microenvironment of myocardial ischemia is detrimental for the transplanted cells mainly due to hypoxia and high free radical concentration [61]. Therefore, preconditioning of MSCs with pharmacological or chemical agents was investigated to improve their therapeutic and regenerative effects. In the present study, MSCs were cultured with L-carnitine, to explore its beneficial role. The main influence of L-carnitine is ATP production and inhibition of apoptosis, by stabilizing the inner mitochondrial membrane, altering membrane potential, and inhibiting mitochondrial splitting [62]. It also enhances the hemodynamic functions and reduces the infarct size, which is consistent with the findings of the present study. A significant reduction of myocardial infarction serum markers; serum CK-MB, and troponin I level, was detected in the groups treated with MSCs, L-carnitine, and L-carnitine-pretreated MSCs, compared with the DOX-treated group which agrees with those reported in previous studies [63,64]. DOX-induced cardiotoxicity can manifest as acute, subacute, or chronic. Acute cardiotoxicity from DOX starts directly following administration, with an incidence rate of presenting echocardiographic abnormalities in around 11% of the patients [13,65]. Therefore, regular monitoring of cardiac biomarkers is essential for patients undergoing DOX treatment to detect early signs of myocardial injury. Various mechanisms of DOX-induced cardiomyopathy were investigated. Oxidative stress, manifested by reactive oxygen species (ROS)-rich microenvironment is a leading

 doi:10.20944/preprints202405.1819.v1

cause of cardiac injury. The cardiomyocytes are highly susceptible to oxidative damage, due to their lower levels of antioxidant enzymes such as peroxidase, catalase, and superoxide dismutase [66]. In agreement with these findings, the current study represented significantly lower levels of the antioxidant enzyme catalase and elevation of the MDA. MDA is a common measure of oxidative stress indicating a significant increase in lipid peroxidation [63]. High levels of oxidative damage devastate the cellular antioxidant defense systems triggering the apoptotic and necrotic cascades [67]. MSCs, particularly under oxidative stress conditions, produce various secretomes that contain cytokines, proteins, growth factors, and exosomes that boost the antioxidant capacity of MSCs. Moreover, under hypoxic conditions, the migration of MSCs is stimulated by chemokine receptor (CXCR7) overexpression through increasing the vascular cells adhesion molecule-1 (VCAM-1) [68]. Specifically, L-carnitine facilitates STAT3 activation and significantly elevates the expression of the antioxidant protein SOD2. In the injured cardiac cells, marked by mitochondrial dysfunction and impaired CaMKII signaling, L-carnitine promotes CaMKII expression and activation, as well as enhances AMPK protein synthesis [69]. Consistent with the mentioned studies, preconditioned-MSCs with L-carnitine revealed the most significant improvement of the cellular antioxidant defense mechanism manifested by MDA and catalase results.

Acute cardiac injury induced by DOX is characterized by cytoplasmic vacuolation and disruption and thinness of myofibrils [70]. Other architecture changes found in the present study demonstrated in the cardiac tissue, following DOX administration, are consistent with several research. They include loss of cardiac muscle fibers, degenerated eosinophilic fibers with pyknotic nuclei, congested blood vessels, fibroplasia, and inflammatory cellular infiltration mainly neutrophils [23,71]. This impairment is associated with a significant inflammatory response revealed by injury of the endothelial cells with leukocyte infiltration and elevation of the inflammatory cytokines; IL-1 β, IL-6, and Tnf-α [72,73 and 65]. Consistent with the previous studies, the current work demonstrated the elevation of the inflammatory mediators; IL-1 β, Tnf-α, NF-κβ, and apoptotic factor; caspase 3 with a decrease of the antiapoptotic factor; Bcl2 in DOX-treated group as documented by Wang et al. [48] and Pakjoo et al. [74]. On the other hand, the L-carnitine-pretreated MSCs group showed the optimum results in decreasing the measured inflammatory, apoptotic, and fibrotic cytokines, and antiapoptotic Bcl2 elevation producing improvement of the structural architecture of cardiac muscles. As approved by previous studies, the influence of MSCs on injured cardiomyocytes involves an intricate interaction of cytokines and signaling pathways. MSCs derive various inflammatory and fibrotic regulators including IL-6, IL-10, TGF-β1, and VEGF which reduce oxidative stress, inhibit inflammation, stimulate cellular regeneration promote proliferation, and prevent apoptosis [75,76]. MSCs reduce the expression of other inflammatory cytokines including interferon-γ (IFN-γ), IL-1β, IL-12, IL-4, and TNF-α. This reduction is achieved by secreting TNF-α stimulated gene/protein 6 (TSG-6), PGE2, and granulocyte-colony stimulating factor (G-CSF). On the other hand, MSCs stimulate the production of anti-inflammatory mediators IL-1, and hepatic nuclear factor-4 alpha (HNF-4α) by increasing the nitric oxide synthase (iNOS) through the activation of the NF-κB pathway [77,78]. In addition to the added antioxidant, anti-inflammatory, and anti-apoptotic role of L-carnitine and its role in the improvement of cardiac tissue architecture {2,42].

Concerning hsp90, a vital molecular chaperone, it regulates various cellular processes such as functional maturation, activation of several proteins, protein folding, and stability [79,80]. For these reasons, hsp90 is overexpressed in several cancers and is believed to aid the maturation of numerous oncoproteins, thereby facilitating cancer growth [81]. In addition, hsp90 was identified in various cardiac injury pathways such as PI3K/AKT (PKB)/mTOR, MAPK, and TNF-α signaling pathways. Therefore, hsp90 plays a significant role in various cardiovascular diseases including atherosclerosis and heart failure [82] as detected in the present study by overexpression in the DOX-treated group and a decrease in its level especially in the L-carnitine pre-treated-MSCs-group. TH regulates the rate of catecholamine synthesis. It is essential for heart function, particularly under stress conditions [83]. TH is a cardiac muscle differentiation that is evident in the initial stages of heart development, especially in gastrulation. Enhanced TH expression resulted in sharp expression of atrial myosin heavy chain (AMHC1) and T-box 5 gene (Tbx5) within the ventricles, indicating an upregulation of

 doi:10.20944/preprints202405.1819.v1

cardiac muscle differentiation markers [84]. Reduction of TH expression in the DOX-treated group and overexpression in the other groups particularly the L-carnitine pre-treated MSCs group together with the same results concerning the proliferative indicators Ki-67 denotes their cardiomyocyte proliferation and differentiation capacities. These findings propose that L-carnitine pretreated-MSCs hold a novel promising treatment for cardiac ischemia and infarction, especially in reducing apoptosis and enhancing cardiac muscle regeneration. Nevertheless, additional research is needed to validate these effects and elucidate the underlying mechanisms.

5. Conclusion

The present study demonstrates that preconditioning mesenchymal stem cells (MSCs) with L-carnitine significantly enhances their therapeutic potential in treating cardiac tissue injury induced by Doxorubicin (DOX). The combined treatment improved key cardiac biomarkers and reduced cardiomyocyte degeneration and necrosis, restoring normal cardiac architecture. These beneficial effects were supported by favorable changes in immunomodulators, proliferative indicators, cardiac differentiation markers, and apoptotic regulators. Thus, L-carnitine pre-treated MSCs represent a promising approach for future stem cell therapy, offering enhanced regenerative and therapeutic outcomes.

Funding: This research received no funding.

Conflicts of interest: The authors declare no conflicts of interest.

Acknowledgment: The Researchers would like to thank the Deanship of Graduate Studies and Scientific Research at Qassim University for financial support (QU-APC- 2024-9/1).

References

1. Anand, S.S.; Islam, S.; Rosengren, A. et al. Risk factors for myocardial infarction in women and men: insights from the INTERHEART study. *Eur Hear J* **2008**, 29, 932-940. doi:10.1093/eurheartj/ehn018
2. Emran, T.; Chowdhury, N.I.; Sarker, M. et al. L-carnitine protects cardiac damage by reducing oxidative stress and inflammatory response via inhibition of tumor necrosis factor-alpha and interleukin-1beta against isoproterenol-induced myocardial infarction. *Biomedicine & Pharmacotherapy* **2021**, 143, 112139, https://doi.org/10.1016/j.biopha.2021.112139.
3. Zhou, M.; Zou, Y.G.; Xue, Y.Z. et al. Long non-coding RNA H19 protects acute myocardial infarction through activating autophagy in mice. *Eur Rev Med Pharmacol Sci* **2018**, 22, 5647-5651. https://doi.org/10.26355/eurrev_201809_15831
4. Zheng, H.F.; Sun, J.; Zou, Z.Y. et al. MiRNA-488-3p suppresses acute myocardial infarction-induced cardiomyocyte apoptosis via targeting ZNF791. *Eur Rev Med Pharmacol Sci* **2019**, 23, 4932–39. https://doi.org/10.26355/eurrev_201906_18083
5. Bajaj, A.; Sethi, A.; Rathor, P. et al. Acute complications of myocardial infarction in the current era: Diagnosis and management. *J Investig Med* **2015**, 63, 844–55. https://doi.org/10.1097/JIM.0000000000000232
6. Russo, I.; Penna, C.; Musso, T. et al. Platelets, diabetes and myocardial ischemia/reperfusion injury. *Cardiovasc Diabetol* **2017**, 16, 71. https://doi.org/10.1186%2Fs12933-017-0550-6
7. Zhao, T.; Chen, S.; Wang, B.C.D. L-Carnitine Reduces Myocardial Oxidative Stress and Alleviates Myocardial Ischemia-Reperfusion Injury by Activating Nuclear Transcription-Related Factor 2 (Nrf2)/Heme Oxygenase-1 (HO-1) Signaling Pathway. *Med Sci Monit* **2020**, 26,e92325.
8. Spetz, J.; Moslehi, J.; Sarosiek, K. Radiation-induced cardiovascular toxicity: mechanisms, prevention, and treatment. *Curr Treat Options Cardiovasc Med* **2018**, 20, 1–1. https://doi.org/10.1007/s11936-018-0627-x
9. Lyon, A. R.; López-Fernández, T.; Couch, L.S. et al. 2022 ESC guidelines on cardio-oncology developed in collaboration with the European Hematology Association (EHA), the European Society for Therapeutic Radiology and Oncology (ESTRO) and the International CardioOncology Society (IC-OS). *Eur. Heart J* **2022**, 43, 4229–4361. https://doi.org/10.1093/eurheartj/ehac244
10. Linders, A. N.; Dias, I. B.; López Fernández, T.; Tocchetti, C. G.; Bomer, N. A review of the pathophysiological mechanisms of doxorubicin-induced cardiotoxicity and aging. *Npj Aging* **2024**, 10(1), 1-9. https://doi.org/10.1038/s41514-024-00135-7
11. Tacar, O.; Sriamornsak, P.; Dass, C. R. Doxorubicin: an update on anticancer molecular action, toxicity and novel drug delivery systems. *J Pharm Pharmacol* **2013**, 65 (2), 157–170. doi: 10.1111/j.2042-7158.2012.01567.x
12. Torre, L.A.; Siegel, R.L.; Ward, E.M.; Jemal, A. Global Cancer Incidence and Mortality Rates and Trends-An Update. *Cancer Epidemiol Biomarkers Prev* **2016**, 25,16–27. https://doi.org/10.1158/1055-9965.epi-15-0578

 doi:10.20944/preprints202405.1819.v1

13. Kong, C.Y.; Guo, Z.; Song, P. et al. Underlying the Mechanisms of Doxorubicin-Induced Acute Cardiotoxicity: Oxidative Stress and Cell Death. *Int J Biol Sci* **2022**, 18(2), 760-770. doi: 10.7150/ijbs.65258.
14. Santos, D.S.; Goldenberg, R.C. Doxorubicin-Induced Cardiotoxicity: From Mechanisms to Development of Efficient Therapy. *Cardiotoxicity*, 1st ed.; Tan, W., InTech; 2018; http://dx.doi.org/10.5772/intechopen.79588
15. Shelburne, N.; Simonds, N.I.; Adhikari, B. et al. Changing Hearts and Minds: Improving Outcomes in Cancer Treatment-Related Cardiotoxicity. *Curr Oncol Rep* **2019**, 21, 9. https://doi.org/10.1007/s11912-019-0751-0
16. Renu, K.; Abilash, V.; Tirupathi Pichiah, P. B.; Arunachalam, S. Molecular mechanism of doxorubicin-induced cardiomyopathy—an update. *Eur J Pharmacol* **2018**, 818, 241–253. doi: 10.1016/j.ejphar.2017.10.043
17. Lee, J.Y.; Chung, J.; Byun, Y.; Kim, K.H.; An, S.H.; Kwon, K. Mesenchymal Stem Cell-Derived Small Extracellular Vesicles Protect Cardiomyocytes from Doxorubicin-Induced Cardiomyopathy by Upregulating Survivin Expression via the miR-199a-3p-Akt-Sp1/p53 Signaling Pathway. *Int J Mol Sci* 2021, 22, 7102. https://doi.org/10.3390/ijms22137102
18. Wenningmann, N.; Knapp, M.; Ande, A.; Vaidya, T.R.; Ait-Oudhia, S. Insights into Doxorubicin-induced Cardiotoxicity: Molecular Mechanisms, Preventive Strategies, and Early Monitoring. *Molecular Pharmacology* **2019**, 96 (2) 219-232. doi: https://doi.org/10.1124/mol.119.115725
19. van der Zanden, S. Y.; Qiao, X.; Neefjes, J. New insights into the activities and toxicities of the old anticancer drug doxorubicin. *FEBS J* **2021**, 288, 6095–6111. https://doi.org/10.1111/febs.15583
20. Jones I.C.; Dass, C.R. Doxorubicin-induced cardiotoxicity: causative factors and possible interventions. *Journal of Pharmacy and Pharmacology* **2022**, 74(12), 1677–1688, https://doi.org/10.1093/jpp/rgac063
21. Chen, X.; Peng, X.; Luo, Y. et al. Quercetin protects cardiomyocytes against doxorubicin-induced toxicity by suppressing oxidative stress and improving mitochondrial function via 14-3-3γ. *Toxicol Mech Methods* **2019**, 29, 344–354. doi: 10.1080/15376516.2018.1564948
22. He, H.; Wang, L.; Qiao, Y. et al. Doxorubicin Induces Endotheliotoxicity and Mitochondrial Dysfunction via ROS/eNOS/NO Pathway. *Front Pharmacol* **2020**, 10,1531. doi: 10.3389/fphar.2019.01531.
23. Abdel-Daim, M. M.; Khalifa, H. A.; Ahmed, A. A. Allicin ameliorates doxorubicin-induced cardiotoxicity in rats via suppression of oxidative stress, inflammation and apoptosis. *Cancer Chemother Pharmacol* **2017**, 80 (4), 745–753. doi: 10.1007/s00280-017-3413-7
24. Fabbri, R.; Macciocca, M.; Vicenti, R. et al. Epigallocatechin-3-gallate inhibits doxorubicin-induced inflammation on human ovarian tissue. *Biosci Rep* **2019**, 39(5), BSR20181424. doi: 10.1042/BSR20181424.
25. Wang, S.; Kotamraju, S.; Konorev, E.; Kalivendi, S.; Joseph, J.; Kalyanaraman, B. Activation of nuclear factor-kappaB during doxorubicin-induced apoptosis in endothelial cells and myocytes is pro-apoptotic: the role of hydrogen peroxide. *Biochem J* **2002**, 367(3), 729-40. doi: 10.1042/BJ20020752.
26. Pakjoo, M.; Ahmadi, S.E.; Zahedi, M. et al. Interplay between proteasome inhibitors and NF-κB pathway in leukemia and lymphoma: a comprehensive review on challenges ahead of proteasome inhibitors. *Cell Commun Signal* **2024**, 22, 105. https://doi.org/10.1186/s12964-023-01433-5
27. Cova, L.; Armentero, M.T.; Zennaro, E. et al. Multiple neurogenic and neurorescue effects of human mesenchymal stem cell after transplantation in an experimental model of Parkinson's disease. *Brain research* **2010**, 1311, 12-27.
28. Karaoz, E.; Okcu, A.; Ünal, Z.S.; Subasi, C.; Saglam, O.; Duruksu, G. Adipose tissue-derived mesenchymal stromal cells efficiently differentiate into insulin-producing cells in pancreatic islet microenvironment both in vitro and in *vivo*. *Cytotherapy* **2013**, 15(5), 557-570.
29. Yang, G.; Fan, X.; Liu, Y. et al. Immunomodulatory Mechanisms and Therapeutic Potential of Mesenchymal Stem Cells. *Stem Cell Reviews and Reports* **2023**, 19(5), 1214-1231. https://doi.org/10.1007/s12015-023-10539-9
30. Van Winkle, A.P.; Gates, I.D.; Kallos M.S. Mass transfer limitations in embryoid bodies during human embryonic stem cell differentiation. *Cells Tissues Organs* **2012**, 196, 34-47 https://doi.org/10.1159/000330691
31. Mayer, A.; Vaupel, P. Hypoxia, Lactate Accumulation, and Acidosis: Siblings or Accomplices Driving Tumor Progression and Resistance to Therapy? *Oxygen Transport to Tissue*, Van Huffel, S.; Naulaers, G.; Caicedo, A.; Bruley, D.F.; Harrison, D.K. *Advances in Experimental Medicine and Biology* 2013, 789. Springer, New York, NY. https://doi.org/10.1007/978-1-4614-7411-1_28
32. Moeinabadi-Bidgoli, K.; Babajani, A.; Yazdanpanah, G. et al. Translational insights into stem cell preconditioning: From molecular mechanisms to preclinical applications. *Biomedicine & Pharmacotherapy* **2021,** 142, 112026, https://doi.org/10.1016/j.biopha.2021.112026.
33. Han, K.; Kim, A.; Kim, M.; Kim, D.; Go, H.; Kim, D. Enhancement of angiogenic effects by hypoxia-preconditioned human umbilical cord-derived mesenchymal stem cells in a mouse model of hindlimb ischemia. *Cell Biol Int* **2016**, 40, 27-35 https://doi.org/10.1002/cbin.10519
34. Noronha, N.; Mizukami, A.; Caliári-Oliveira, C. et al. Priming approaches to improve the efficacy of mesenchymal stromal cell-based therapies. *Stem Cell Res Ther* **2019**, 10, 131. https://doi.org/10.1186/s13287-019-1224-y

35. Kahrizi, M.S.; Mousavi, E.; Khosravi, A. et al. Recent advances in pre-conditioned mesenchymal stem/stromal cell (MSCs) therapy in organ failure; a comprehensive review of preclinical studies. *Stem Cell Res Ther* **2023**, 14, 155. https://doi.org/10.1186/s13287-023-03374-9
36. Longo, N; Frigeni, M.; Pasquali, M. Carnitine transport and fatty acid oxidation. *Biochim Biophys Acta* **2016**, 1863(10), 2422-35. doi: 10.1016/j.bbamcr.2016.01.023.
37. Thakur, Y.; Bharti, R.; Sharma, R. Myths and reality of L-carnitine (3-Hydroxy 4-N trimethylammonium butyrate) supplementation and its chemistry: A systematic review, *Materials Today: Proceedings* 2022, 48(5), 1277-1282. https://doi.org/10.1016/j.matpr.2021.08.287.
38. Mohamed, E.; Reda, A.; Elnegris, H. Role of L-carnitine Treated Mesenchymal Stem Cells on Histological Changes in Spleen of Experimentally Induced Diabetic Rats and the Active Role of Nrf2 Signaling. *Egyptian Journal of Histology* **2021**, 44(3), 630-642. doi:10.21608/ejh.2020.34159.1323
39. Fathi, E.; Farahzadi, R.; Charoudeh, H.N. L-carnitine contributes to enhancement of neurogenesis from mesenchymal stem cells through Wnt/β-catenin and PKA pathway. *Exp Biol Med* **2017**, 242(5), 482-486. doi: 10.1177/1535370216685432.
40. Mobarak, H.; Fathi, E.; Farahzadi, R.; Zarghami, N.; Javanmardi, S. L-carnitine significantly decreased aging of rat adipose tissue-derived mesenchymal stem cells. *Vet Res Commun* **2017**, 41, 41-47. https://doi.org/10.1007/s11259-016-9670-9
41. Farag, A.; Elfadadny, A.; Mandour, A.S. et al. Potential protective effects of L-carnitine against myocardial ischemia/reperfusion injury in a rat model. *Environ Sci Pollut Res* **2024**, 31, 18813–18825. https://doi.org/10.1007/s11356-024-32212-5
42. Xue, M.; Chen, X.; Guo, Z. et al. L-Carnitine Attenuates Cardiac Dysfunction by Ischemic Insults Through Akt Signaling Pathway. *Toxicological Sciences* **2017**, 160(2), 341–350, https://doi.org/10.1093/toxsci/kfx193
43. El Sadik, A.; El Ghamrawy, T.A.; Abd El-Galil, T.I. The Effect of Mesenchymal Stem Cells and Chitosan Gel on Full Thickness Skin Wound Healing in Albino Rats: Histological, Immunohistochemical and Fluorescent Study. *PLoS ONE*, **2015** 10(9), e0137544. https://doi.org/10.1371/journal.pone.0137544
44. Abdelhafez, D.; Aboelkomsan, E.; El Sadik, A. O. et al. The Role of Mesenchymal Stem Cells with Ascorbic Acid and N-Acetylcysteine on TNF-α, IL 1β, and NF-$\kappa\beta$ Expressions in Acute Pancreatitis in Albino Rats. *Journal of Diabetes Research* **2021**, 6229460, https://doi.org/10.1155/2021/6229460
45. Elzainy, A.; El Sadik, A.; Altowayan, W.M. Comparison between the Regenerative and Therapeutic Impacts of Bone Marrow Mesenchymal Stem Cells and Adipose Mesenchymal Stem Cells Pre-Treated with Melatonin on Liver Fibrosis. *Biomolecules* **2024**, *14*, 297. https://doi.org/10.3390/biom14030297
46. Oliveira, M.S.; Melo, M.B.; Carvalho, J.L. et al. Doxorubicin Cardiotoxicity and Cardiac Function Improvement After Stem Cell Therapy Diagnosed by Strain Echocardiography. *J Cancer Sci Ther* **2013**, 5(2), 52-57. doi: 10.4172/1948-5956.1000184.
47. Kolmanová, E.; Bartošová, L.; Khazneh, E.; Parák, T.; Suchý, P. Comparison of the specificity of cardiac troponin I and creatine kinase MB in isoproterenol-induced cardiotoxicity model in rats. *Acta Vet Brno* **2015**, 84: 343–350. doi:10.2754/avb201584040343
48. Wang, Q.; Cui, Y.; Lin, N.; Pang, S. Correlation of cardiomyocyte apoptosis with duration of hypertension, severity of hypertension and caspase-3 expression in hypertensive rats. *Exp Ther Med* **2019**, 17(4), 2741-2745. doi: 10.3892/etm.2019.7249.
49. Zhang, Y.; Chiu, S.; Liang, X. et al. Rap1-mediated nuclear factor-kappaB (NF-κB) activity regulates the paracrine capacity of mesenchymal stem cells in heart repair following infarction. *Cell Death Discovery* **2015**, 1, 15007. https://doi.org/10.1038/cddiscovery.2015.7
50. Harouki, N.; Nicol, L.; Remy-Jouet, I. et al. The IL-1β Antibody Gevokizumab Limits Cardiac Remodeling and Coronary Dysfunction in Rats With Heart Failure. *J Am Coll Cardiol Basic Trans Science* **2017**, 2 (4), 418–430. https://doi.org/10.1016/j.jacbts.2017.06.005
51. Liu, J.; Yeo, H.C.; Doniger, S.J.; Ames, B.N. Assay of aldehydes from lipid peroxidation: Gas chromatography-mass spectrometry compared to thiobarbituric acid. *Anal. Biochem* **1997**, 245,161–165. doi: 10.1006/abio.1996.9990.
52. Aebi, H. Catalase in vitro. *Methods in Enzymol* **1984**, 105, 121 – 126. https://doi.org/10.1016/S0076-6879(84)05016-3
53. El Sadik, A.; Mohamed, E.; Elzainy, A. Postnatal changes in the development of rat submandibular glands in offspring of diabetic mothers: Biochemical, histological and ultrastructuralstudy. *PLoS ONE* **2018**, 13(10), e0205372. https://doi.org/10.1371/journal.pone.0205372
54. El Aasar, H.; Rashed, L.; El Sadik A.; Amer, R.; Emam, H. (2021). The role of the adipose tissue-derived mesenchymal stem cells enriched with melatonin on pancreatic cellular regeneration. *Folia Morphologica* **2021**, #84579 2021 doi: 10.5603/FM.a2021.0093
55. Armitage, P.; Berry, G. Statistical methods in medical research, 3rd ed., 1994, Blackwell Scientific Publications, London.

56. Guijarro, D.; Lebrin M.; Lairez O. et al. Intramyocardial transplantation of mesenchymal stromal cells for chronic myocardial ischemia and impaired left ventricular function: Results of the MESAMI 1 pilot trial. *Int J Cardiol* **2016**, 209, 258–265. doi: 10.1016/j.ijcard.2016.02.016.
57. Butler, J.; Hamo, C.E.; Udelson, J.E. et al. Reassessing Phase II Heart Failure Clinical Trials: Consensus Recommendations. *Circ Heart Fail* **2017**, 10, e003800. doi: 10.1161/CIRCHEARTFAILURE.116.003800.
58. Razeghian-Jahromi, I.; Matta, A.G.; Canitrot, R. et al. Surfing the clinical trials of mesenchymal stem cell therapy in ischemic cardiomyopathy. *Stem Cell Res*, **2021**, 12,361. doi: 10.1186/s13287-021-02443-1.
59. Kuraitis, D.; Giordano, C.; Ruel, M.; Musaro, A.; Suuronen, E.J. Exploiting extracellular matrix-stem cell interactions: A review of natural materials for therapeutic muscle regeneration. *Biomaterials*, **2012**, 33, 428–443. doi: 10.1016/j.biomaterials.2011.09.078.
60. Khubutiya, M.S.; Vagabov, A.V.; Temmov, A.A.; Sklifas, A.N. Paracrine mechanisms of proliferative, anti-apoptotic and anti-inflammatory effects of mesenchymal stromal cells in models of acute organ injury. *Cryotherapy* **2014**, 16, 579–585. doi: 10.1016/j.jcyt.2013.07.017.
61. Brodarac, A.; Šarić, T.; Oberwallner, B.; Mahmoodzadeh, S.; Neef, K.; Albrecht, J. Susceptibility of murine induced pluripotent stem cell-derived cardiomyocytes to hypoxia and nutrient deprivation. *Stem Cell Res* **2015**, 6,83. doi: 10.1186/s13287-015-0057-6.
62. Fathi, E.; Farahzadi, R. Application of L-carnitine as nutritional supplement in veterinary medicine. *Rom J Biochem* **2014**, 51(1), 31-41
63. Hadi, N.; Yousif, N.G.; Al-amran, F.G. et al. Vitamin E and telmisartan attenuates doxorubicin induced cardiac injury in rat through down regulation of inflammatory response. *BMC Cardiovasc Disord* **2012**, 12, 63. https://doi.org/10.1186/1471-2261-12-63
64. Abbas, N.A.T.; Kabil, S.L. Liraglutide ameliorates cardiotoxicity induced by doxorubicin in rats through the Akt/GSK-3β signaling pathway. *Naunyn-Schmiedeberg's Arch Pharmacol* **2017**, 390, 1145–1153. https://doi.org/10.1007/s00210-017-1414-z
65. Dulf, P.L.; Mocan, M.; Coadă, C.A. et al. Doxorubicin-induced acute cardiotoxicity is associated with increased oxidative stress, autophagy, and inflammation in a murine model. *Naunyn Schmiedebergs Arch Pharmacol* **2023**, 396(6), 1105-1115. doi: 10.1007/s00210-023-02382-z.
66. Pereira, G.C.; Silva, A.M.; Diogo, C.V.; Carvalho, F.S.; Monteiro, P.; Oliveira, P.J. Drug-induced cardiac mitochondrial toxicity and protection: from doxorubicin to carvedilol. *Curr Pharm Des* **2011**, 17,2113–2129. doi: 10.2174/138161211796904812.
67. Ayala, A.; Muñoz, M.F.; Argüelles, S. Lipid peroxidation: production, metabolism, and signaling mechanisms of malondialdehyde and 4-hydroxy-2-nonenal. *Oxid Med Cell Longev* **2014**, 2014, 360438. doi: 10.1155/2014/360438.
68. Liu, L.; Chen, J.X.; Zhang, X.W. et al. Chemokine receptor 7 overexpression promotes mesenchymal stem cell migration and proliferation via secreting Chemokine ligand 12. *Sci Rep* **2018**, 8, 204. https://doi.org/10.1038/s41598-017-18509-1.
69. Vacante, F.; Senesi, P.; Montesano, A.; Frigerio, A.; Luzi, L.; Terruzzi, I. L-Carnitine: An Antioxidant Remedy for the Survival of Cardiomyocytes under Hyperglycemic Condition. *J Diabetes Res* **2018**, 9, 2018, 4028297. doi: 10.1155/2018/4028297.
70. Tomita, S.; Ishida, M.; Nakatani, T. et al. Bone marrow is a source of regenerated cardiomyocytes in doxorubicin-induced cardiomyopathy and granulocyte colony-stimulating factor enhances migration of bone marrow cells and attenuates cardiotoxicity of doxorubicin under electron microscopy. *J Heart Lung Transplant* **2004**, 23, 577–84. doi: 10.1016/j.healun.2003.06.001.
71. Ibrahim A.A.; Abdo S.A.M.; Anas, S. et al. Mesenchymal Stem Cell Therapy for Doxorubicin-Induced Cardiomyopathy: Potential Mechanisms, Governing Factors, and Implications of the Heart Stem Cell Debate. *Frontiers in Pharmacology* **2019**, 10. doi=10.3389/fphar.2019.00635
72. Pecoraro, M.; Del Pizzo, M.; Marzocco, S. et al. Inflammatory mediators in a short-time mouse model of doxorubicin-induced cardiotoxicity. *Toxicol Appl Pharmacol* **2016**, 293, 44–52. 10.1016/j.taap.2016.01.006
73. Jiang, Y.; Zhang, Q. Catalpol ameliorates doxorubicin-induced inflammation and oxidative stress in H9C2 cells through PPAR-γ activation. *Exp Ther Med* **2020**, 20, 1003–1011. doi: 10.3892/etm.2020.8743.
74. Pakjoo, M.; Ahmadi, S.E.; Zahedi, M. et al. Interplay between proteasome inhibitors and NF-κB pathway in leukemia and lymphoma: a comprehensive review on challenges ahead of proteasome inhibitors. *Cell Commun Signal* **2024**, 22(1),105. doi: 10.1186/s12964-023-01433-5.
75. Chan, B.; Wong, W.; Lee, M.L. et al. Exosomes in Inflammation and Inflammatory Disease. *Proteomics* **2019**, 19, e1800149.
76. Zhou, C.; Zhang, B.; Yang, Y. et al. Stem cell-derived exosomes: Emerging therapeutic opportunities for wound healing. *Stem Cell Res Ther* **2023**, 14, 107.
77. Ye, Z.; Lu, W.; Liang, L. et al. Mesenchymal stem cells overexpressing hepatocyte nuclear factor-4 alpha alleviate liver injury by modulating anti-inflammatory functions in mice. *Stem Cell Res Ther* **2019**, 10, 149. https://doi.org/10.1186/s13287-019-1260-7.

78. Cruz-Barrera, M.; Flórez-Zapata, N.; Lemus-Diaz, N. et al. Integrated Analysis of Transcriptome and Secretome from Umbilical Cord Mesenchymal Stromal Cells Reveal New Mechanisms for the Modulation of Inflammation and Immune Activation. *Front Immunol* **2020**, 11, 575488. https://doi.org/10.3389/fimmu.2020.575488.
79. Luengo, T.; Mayer, M.P.; Rudiger, S.G.D. The Hsp70-Hsp90 Chaperone Cascade in protein folding. *Trends Cell Biol*. **2019**, 29,164–77. doi: 10.1016/j.tcb.2018.10.004.
80. Cabaud-Gibouin, V.; Durand, M.; Quere, R.; Girodon, F.; Garrido, C.; Jego, G. Heat shock proteins in leukemia and lymphoma: multitargets for innovative therapeutic approaches. *Cancers* **2023**, 15, 984.
81. Liu, L.; Deng, Y.; Zheng, Z. et al. Hsp90 inhibitor STA9090 sensitizes Hepatocellular Carcinoma to Hyperthermia-Induced DNA damage by suppressing DNA-PKcs protein Stability and mRNA transcription. *Mol Cancer Ther* **2021**, 20, 1880–92.
82. Qi, S.; Yi, G.; Yu, K.; Feng, C.; Deng, S. The Role of HSP90 Inhibitors in the Treatment of Cardiovascular Diseases. *Cells* **2022**, 11(21), 3444. doi: 10.3390/cells11213444.
83. Nisimura, L.M.; Bousquet, P.; Muccillo, F.; Tibirica, E.; Garzoni, L.R. Tyrosine hydroxylase and β2-adrenergic receptor expression in leukocytes of spontaneously hypertensive rats: putative peripheral markers of central sympathetic activity. *Braz J Med Biol Res* **2020,** 53(12),e9615. doi: 10.1590/1414-431X20209615.
84. López-Sánchez, C.; Bártulos, O.; Martínez-Campos, E. et al. Tyrosine hydroxylase is expressed during early heart development and is required for cardiac chamber formation. *Cardiovascular Research* **2010**, 88(1),111-120. doi: 10.1093/cvr/cvq179.